Journal of Harbin Engineering University Vol 44 No. 8
ISSN: 1006-7043 August 2023

Investigation of Compressive Properties of Mn/Mg Reinforced Close-Cell Aluminium Metal Foam

Kulwant Kaur [a,*], Sunil Kumar [b], and Deepak Bhandari [b]
[a] M.Tech Student*, [b] Assistant Professor
[a, b] Mechanical Engineering Section, Yadavindra Department of Engineering,
Punjabi University Guru Kashi Campus, Talwandi Sabo, Bathinda, Punjab, 151302, India

Abstract: The work presented in this paper is based on the enhancement of the mechanical properties of the aluminium base closed-cell metal foam through the addition of reinforcing particles in different percentages. Closed-cell aluminium foams with the addition of Mn (1% by weight) and Mg (1.5%, 2%, and 2.5% by weight) are successfully prepared by the melt route method. In this process, Ca (2% by weight) is used as a thickening agent and $CaCO_3$ (1% by weight) as a foaming agent. The morphology and mechanical behaviour of Al-based metal foam have been examined to investigate the impact of reinforcing elements. It has been concluded that the addition of reinforcing elements initially helped to increase the compressive strength as found in foam-1, but further addition of Mg did not have any beneficial effects. It has been found that the value of compression strength strongly depends on foam density and can be depicted by finding the ratio of yield strength to density. The higher value of the ratio of yield strength to density depicts a better-quality metal form. The results show that the ratio of yield strength to density for foam-0, foam-1, foam-2 and foam-3 in comparison to form-0 is found to be 1.00, 1.35, 1.007 and 0.59. So this can be concluded that foam-1 possesses the highest compressive strength among all forms under investigation. The addition of reinforcing elements increases the length of the plateau which increases the energy absorption. It is found that proper bonding of reinforcing particles helps in improving energy absorption. It is also found that besides the increase in density and variations in pores uniformity, foam-1 is found to be superior among all other foams. By fixing the percentage of Mn by 1 wt%, the best results are obtained by adding 1.5 wt. % Mg in the melt.

Keywords: Aluminium Foam, Foaming, Blowing Agent, Melt Route, Porosity, Microstructure, Strength-to-weight Ratio, Foaming Efficiency, Density, Energy Absorption, Strength.

1 Introduction

Aluminium foam is a cellular structure of solid aluminium with gas-filled pores. The foams are an appealing structural material that can mimic the mechanical properties of foams found in nature, like wood or bones. The main characteristics of aluminium foams are efficient energy absorption, excellent stiffness-to-weight ratio, Low thermal conductivity, Fire resistance, Shock wave attenuation, and Sound and vibration damping [1, 2, 3]. The aluminium foam can be classified as open and closed cell forms. Open-cell metal foams, also known as metal sponges, can be produced using powder metallurgy or foundries. To create foam using the powder method, space holders are required [4, 5]. As the name implies, they provide room for open pores during or after foam creation. Foams are created using copies of the pattern open-celled polyurethane foams that are used as a skeleton in foundry processes [4, 5]. In closed-cell metal foam, the pores are sealed. Closed-cell metal foams have been developed by foaming light metals by inert gas injection or using a blowing agent [5]. They are light & stiff and are frequently proposed as a lightweight structural material.

2 Manufacturing Of Aluminium Foam

Aluminium melts are generally foamed by creating gas bubbles in the liquid provided that the melt has been prepared such that the emerging foam is fairly stable during processing. This can be done by adding fine ceramic powders or alloying elements to the melt which foam stabilizing particles, or by other means [6, 7]. There are many ways to manufacture cellular metallic materials. Some methods are similar to techniques used for foaming aqueous or polymer liquids; whereas others are specially designed by taking advantage of characteristic properties of metals such as their

sintering activator and the fact that they can be electrically deposited [7].

General properties [11, 12] of aluminium metal foams include very high porosity and strength, retention of physical properties of their base material, lightweight and stiff structural materials, foam properties disappearing after maximum compression, and fire resistance. The mechanical properties of the pure aluminium foam are Density=0.11 to 0.27 g/cm3, Maximum service temperature=450°C, Melting point=660°C, Compression Strength=2.53 MPa, Tensile Strength=1.24 MPa, Shear Strength=1.31 MPa, Modulus of Elasticity=103.08 MPa, and Specific Heat=0.895 J/g-C. Various methods can be classified according to the state the metal is processed. Figure 4 shows the classification of foam manufacturing processes [7].

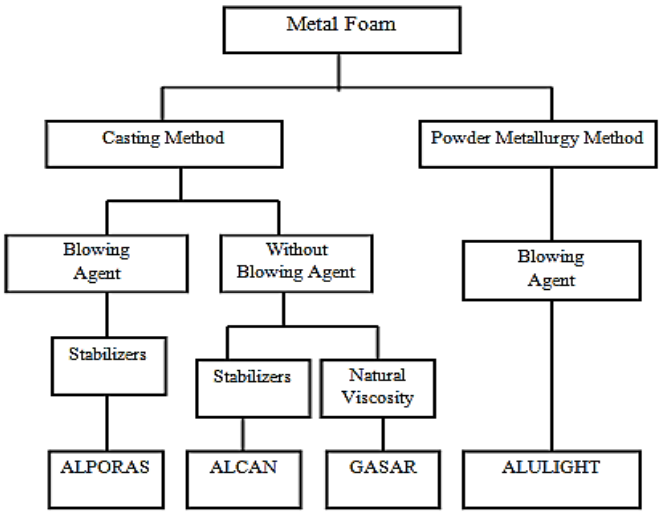

Figure 4: Foam manufacturing processes [7]

2 Metal Foaming Process

2.1 Foaming by Gas Injection

This method uses silicon carbide, aluminium oxide, or magnesium oxide particles to increase the melt viscosity [7]. As a result, the first step entails creating an aluminium melt containing these ingredients. To ensure a uniform distribution of particles, this step reportedly calls for some advanced mixing methods [7]. In a subsequent step, the melt is foamed by injecting gases into it with the help of specialized rotating impellers or vibrating nozzles. These cause the melt to produce uniformly distributed, extremely tiny gas bubbles [7]. Due to the high viscosity of the melt, the resulting viscous mixture of bubbles and melt floats to the liquid surface where they are unable to escape and eventually condense into a relatively dry liquid foam as the liquid metal drains out. Due to the inclusion of ceramic particles in the melt, the foam is stable [7].

2.2 Foaming by Powder Compacts

Metal powders can be used to create foamed metals. To create dense, metal powders and metal powder blends, it must first be combined with a blowing agent [8]. A suitable compaction method is used to add the blowing agent into the metal matrix without any discernible residual open porosity [8]. Thereafter, the precursor is manufactured to counter the presence of any residual porosity. The next step is a heat treatment at a temperature close to the matrix material melting point. The evenly dispersed blowing agent, present in the dense metallic matrix, disintegrates. The melting precursor material is forced to expand by the released gas, creating a highly porous structure.

2.3 Foaming with Blowing Agents

This way for foaming melts directly is to add a powdered blowing agent to the melt instead of injecting gas into it. The blowing agent decomposes under the influence of heat and releases gas which then propels the foaming process [9]. Initially, the viscosity-enhancing agent is added to the melt. The

melt is then stirred to increase its viscosity. The blowing agent is then added that releases gas in the hot viscous liquid. The gas bubbles formed tend to rise to the surface of the melt but due to high viscosity their movement is slowed down and they get trapped inside the melt. Then the melt soon starts to expand slowly and further gradually fills the foaming vessel. After cooling the vessel below the melting point of the alloy, the liquid foam turns into a solid and can be taken out of the mould for further processing. To produce metal foam, hydrides and carbonates are used as blowing agents.

3 Literature Review

The use of metal foams in manufacturing has become a promising area of research in recent periods. Relevant research papers for applications of aluminium foams in manufacturing are discussed in the following paragraphs.

Kováèik [10] investigated the performance of steel tubes made in zinc and aluminium foam. The authors found that better performance was obtained with zinc foams when the foams were prepared by directly foaming in the profile. Aluminium foaming in steel tubes causes substantial structural changes to the profile material that harm its mechanical propertie**s.** Results showed that the use of foamed stiffeners is effective when the profiles are foamed in the weakest sections. Esen and Bor [11] investigated the properties of titanium foams produced using magnesium powders as spacer particles. The production of titanium foams with porosities between 45% and 70% and an average pore size of 5 mm took place. At a cross speed of 0.5 mm/min, compression tests were performed using the universal tension-compression machine. The authors concluded that the elastic moduli and yield strength have laid within safe limits.

Haesche et al. [12] used dolomite powders as a foaming agent to successfully replace TiH_2 powder, fabricated by milling of natural minerals. Dolomite powder particles were regularly included in different volume portions of foaming precursors prepared either through powder metallurgy or the melt route. Based on experimental results, it has been found that the porosity of aluminium foam significantly affects its properties, making it possible to tailor the desired property by choosing the density of the foam. Neu et al. [13] produced Mg and Mg-Al alloy foams with 60–70% porosity. Among all the conditions tested, pure Mg foams with good expansion and satisfactory foam structure could only be produced from extruded samples containing TiH_2 and pressure-induced foaming. All the Mg-Al alloys prepared by extrusion yielded good foam structure only when PIF was applied, not by foaming at ambient pressure.

Cambronero et al. [14] used calcium carbonate as a foaming agent for use in the melt route. Due to the smaller particle size, manufacturing variables like powder mixing time, hot extrusion pressure, and foaming time are reduced. Foam development with minimal aluminium drainage is made possible by partial calcium carbonate decomposition. It was concluded that uniaxial compressive properties are slightly better when marble is used instead of synthetic calcium carbonate. Li et al. [15] investigated the control of the process parameters for the production of closed-cell aluminium foam with a uniform cell structure and high porosity. The authors used foaming agents such as calcium addition, ZrH_2 content, and parameters such as experimental temperature, and stirring and holding time in this experimentation. It was found that with 0.6 to 1.2 percent ZrH_2, the average pore size and porosity hardly change, whereas they rise with rising foaming temperature and exhibit an essentially linear relationship with calcium addition.

Kevorkian [16] investigated the effect of replacing TiH_2 powder as a foaming agent with commercial $CaCO_3$ powders of different average particle sizes. The authors used powder metallurgical and melt routes to prepare foaming precursors with various proportions of $CaCO_3$ powder particles as a foaming agent. Authors attained approximately 99% theoretical densities in precursors made by the PM route that contained 3-7 vol. percent of $CaCO_3$ particles with an average particle size of 38 μm. It has been concluded that for the range of foam densities analyzed, the compression strength was found to be superior in samples with increased density (0.55 g/cm_3) and hence lower foaming efficiency (79.6).

Tajally et al. [17] investigated the effect of cold rolling operations performed on aluminum-based

precursors made by hot continuous extrusion from powder on its foaming ability. It was found that the foaming ability significantly improved with the present investigations. It has been found that the total amount of rolling reduction used has no bearing on the increase in foamability of cold rolling. Byakova et al. [18] investigated the advantages of conventional titanium hydride-coated $CaCO_3$ closed cell foam by melt route. It was found that the investigated foam possessed very good mechanical performance due to finely cellular structure and remarkable improvement of the cell wall microstructure. The authors found that the mean cell size of $CaCO_3$ foam is at least two times smaller than TiH_2 foam. The presence of a high fraction volume of brittle constituents reduces the wall ductility and toughness of TiH_2 foam compared to $CaCO_3$ foam.

Onsalung et al. [19] revealed the failure characteristic of foam-filled tubes. It was found that as foam density increases, the number of folds in deformed tubes increases. The outcome also suggests that the tube tends to absorb more energy as foam density rises. However, the results show that the 200 kg/m^3 foam-filled tube offers the highest specific energy absorption when taking structural weight into account. Kenny et al. [20] discussed that aluminium foam material has unique properties with low density, high damping capacity, high permeability, high sound absorptivity and is non-flammable. The authors investigated the deformation behaviour of a crash box from a racing car during a head-on collision in a virtual environment. It has been concluded that the mechanical properties of aluminium foam make it very useful for use in automobile applications.

Hussain and Suffin [21] determined the effect of NaCl space holder content on the morphology and compression properties of aluminium foam. It was possible to create aluminium foam with a porosity of 20–70% and an average pore size of 400–500 m. Because the foam structure collapsed under greater strain during compression loading, foam made with 60 wt.% NaCl has the highest energy absorption. However, due to brittleness brought on by lingering NaCl particles, 80 wt.% NaCl produced the foam with the lowest compressive characteristics and energy absorption. Mohan et al. [22] studied the effect of impact loading on sample blocks with aluminium foam core and various face sheets including Al, SS, and CFRP with a velocity of 6.7 m/s. Blocks with SS face sheets absorbed almost all the impact energy and best choice as an energy absorber in comparison with blocks with other face sheet materials. It was found that the foam's energy-absorbing capacity increased with foam thickness.

Shiomi and Tanino [23] proposed the combined process of hot power extrusion and molding to produce aluminium foams directly from powder. The aluminium foam was injected into the mold by extruding A6061 aluminium powder combined with TiH2 powder through a die heated above the melting point. It was discovered that friction and gravity have an impact on foam molding effect of gravity is significant when a large step exists at the connection between the mold inlet and the die outlet, and friction is dominant in cases where foam is molded in a narrow space. Paulin et al. [24] found that foaming aluminium by powder compaction method gives better foaming results with a good green density of up to 98%. Though, it is practically impossible to achieve green densities higher than 96% with AlSi12 powder. It was concluded that higher green densities can be achieved by increasing the compacting pressure and/or pre-heating the precursors to increase their compressibility.

Crupi et al. [25] investigated the impact behaviour of aluminium foam sandwiches through experimental tests based on the energy balance model. The model parameters were obtained from the measurements carried out on the CT images of the impacted panels and not from the results of static tests, as is usually done in the literature. The failure mode and the damage have been investigated by computed tomography. Low-velocity impact tests on AFS structures have shown that the dynamic response of these sandwiches depends on the quality and mechanical properties of the foam core material. Haidar et al. [26] compared the uniaxial compressive modulus and strength of the developed aluminium metal matrix composite foam with existing models for metal foams. It was shown that there exists a greater deviation between the experimental and theoretical values like modulus and strength in the elastic region. The reason behind this is

imperfection, cell size, and randomness inside the porous structure.

Ghosh et al. [27] introduced $CaCO_3$ along with Titanium hydride in the process of foam preparation in the liquid metallurgy route. Investigations into acoustic absorption characterization revealed that the developed Al-MMC foam has excellent sound absorption properties and is comparable with other good sound-absorbing materials. Applications such as fire-resistant structures, heat exchangers, and sound absorbers in automobile industries like front bumper and exhaust were also discussed. Matijasevic-Lux et al. [28] used titanium hydride for foaming the aluminium casting alloy $AlSi_6Cu_4$. To improve foaming characteristics, the TiH_2 powder was subjected to various heat treatments before processing. Untreated and pre-treated powders were characterized by oxygen analysis and thermal analysis applying various temperature profiles, X-ray diffraction, and transmission electron microscopy. In addition, foaming trials were carried out based on various TiH_2 powders. It was found that the oxidation of TiH_2 particles is responsible for the shift in decomposition temperature.

Marchi and Mortensen [29] studied the mechanical properties of high-purity aluminium foams produced by replication from salt precursors measured in compression. These foams have homogeneous open-porosity, cell sizes equivalent to the particle size of the precursor salt, and relative densities of nearly 25%. Deformation is uniform and strain hardening similar to the bulk material is observed without plateau stress. Smith et al. [30] fabricated aluminium foam/dense steel composites by friction stir welding. It was shown that although heat treatment of the precursor evolved a brittle intermetallic compound layer, the bonding strength of the interface consisting of the intermetallic compound layer was relatively high compared with the fracture strength of the aluminium foam.

Banhart [31] studied the effect of solid inclusions on foam stability and concluded that solid inclusions are influencing foam stability through their wetting behaviour, their shape, and their distribution in the melt (network formation, clustering, or segregation). Besides the particle concentration and size, recent investigations showed that the compositions of both the metallic melts and the stabilizing particles influence stability. Hangai et al. [32] fabricated aluminium foam/dense steel composites by friction stir welding. It was shown that although heat treatment of the precursor evolved a brittle intermetallic compound layer, the bonding strength of the interface was relatively high compared with the fracture strength of the aluminium foam.

Li et al. [33] investigated that SiCp/2024Al composite foams were successfully manufactured by powder metallurgical methods using the foaming agent $CaCO_3$. The pore diameter and porosity increase first and decrease later with increasing the foaming agent content. The pore diameter and porosity decrease with increasing the SiC particle content. The presence of SiC particles can improve liquid foam stabilization. Zhou et al. [34] successfully manufactured copper foam using calcium carbonate as a blowing agent. The effect of copper particle size and compacting pressure on the porosity of porous samples is analyzed. It was found by the authors that the compressive strength and electrical conductivity of copper foams decrease with the porosity. The thermal expansion coefficient of copper foams increases when the temperature rises

Xia et al. [35] fabricated closed-cell aluminium foams with different Mn contents by the melt-foaming method using Ca as a thickening agent and TiH_2 as a foaming agent. The effects of Mn elements on the compressive properties of Al foams were studied. The results showed that the distribution of Mn elements was uniform in the cell walls. They were mainly distributed in the cell wall matrix in the form of MnO_2, Al_6Mn intermetallic, Al–Mn solid solutions and un-dissolved Mn particles. The addition of Mn elements improved the micro-hardness, plateau region compressive strength, and yield stress of the foams. Yang et al. [36] fabricated close-cell Cu-Mg alloy foam by using the powder metallurgy technique. In their study, they have taken pure Cu powder and Mg powder to fabricate foam by using CaCO3 as a blowing agent. The key to developing successful metal foam is to form an intermetallic compound ($Mg_2Cu/MgCu_2$) which should have a lower melting temperature by sintering treatment. They found that the prepared foam was brittle but Mg in the foam matrix is beneficial for increasing the compressive strength.

Liu et al. [37] developed Al-Si-SiC composite foam by melt route method and performed the compression test at elevated temperatures and found the brittle compressive behaviour of foam at room temperature as well as at elevated temperatures. The material of the cell wall has a significant effect on compressive properties and energy absorption characteristics, which can be obtained by adding the appropriate particles in optimum percentage into the parent metal. Kumar and Pandey [38] prepared LM-13 alloy foams via the melt route method using pre-treated $CaCO_3$ at 300^0C as a blowing agent. The study was conducted for optimizing the various parameters like melt temperature, size and amount of blowing agent, and stirring time for producing uniform-size foams. It was observed that the distribution of the blowing agent depends upon the viscosity of the melt and stirring speed.

Choi et al. [39] studied the compression and wear behaviour of freeze-cast Ti and Ti5W alloy foams, which were further predicted by an analytical model and compared with experimental results for finding suitability in biomedical applications. Sharifi et al. [40] checked the dry sliding wear behaviour of open-cell Al-Mg/Al2O3 and Al-Mg/SiC-Al2O3 composite pre-foams and found that the wear behaviour depended on the density and pores per inch. The results showed that lower wear rates were obtained with smaller cell sizes and higher densities. Bisht and Gangil [40] prepared Al metal foam by adding Zn particles in different weight percentages and demonstrated a significant improvement in compression strength due to the uniform distribution of Zn particles in the cell wall matrix. It was proposed that zinc-containing foams possess higher compressive strength and energy absorption capacities as compared to pure aluminium foams. It was also concluded that an increase in the percentage of Zn particles helps to increase the compressive strength, plateau region, and energy absorption, in addition to providing better and uniform pores.

Bisht et al. [41] prepared closed-cell aluminium metal foam with the addition of Zn and Mg through the melt route method. Mechanical and sliding behaviour was observed. It was found that the compressive strength increases with an increase in the weight percent addition of magnesium in Al with the characteristics of the plateau region becoming flatter and longer. Ghaleh et al. [42] prepared A356 Close cell aluminium foam through the melt route method only by using $CaCO_3$ as a blowing agent. The density of the foam was ranging from 0.32g/cm^3 to 0.46g/cm^3 and the cell size ranged between 1.5mm to 3.1mm. The compressive properties and energy absorption properties increase with an increase in relative densities.

4 Problem Formulation

4.1 Material Selection

From the literature survey, it has been found that metal foam due to its high stiffness to bending ratio and good absorption energy can be successfully used as a structural material. They also possess a high damping capacity and thus can be used in the construction of places where better communication is required [4, 5]. Also, the main advantage which metal foam offers us it's its ultra-low density which lies in the range of 0.2-0.6 g/cm^3. Aluminium foam can be foamed under ambient conditions at a low melting point. However, a good structural material should possess high compressive strength [4, 5]. Table 1 shows the compressive strength of different foams.

Table 1: Compressive strength of different metal foams [4, 5, 25, 32, 40]

Sr	Material	Blowing agent	Porosity	Compression strength	Reinforcing agent
1	Titanium	Argon gas	45-69.8%	15-116 MPa	Alumino-silicate
2	Copper	K_2CO_3	60-70%	30 MPa (60%)	Alumino-silicate
3	Carbon	Sodium bicarbonate	65-70%	3.78, 0 wt.% 4.56, 3 wt.% 5.48, 7 wt.% 6.39 11 wt.% 4.71 15 wt.%	Alumino-silicate
4	Aluminium	TiH_2	79.95%	2.68MPa	Manganese

		$CaCO_3$	79%	5.12MPa	
5	Aluminium	TiH_2	79.95%	4.68MPa (0.2 wt. %)	Manganese
6	Magnesium	$CaCO_3$	53-71.1%	8.69-21MPa	Alumino-silicate

From Table 1 it is clear that titanium has very good compression strength but its density in comparison to aluminium and magnesium is quite high [4, 5]. Magnesium being lighter than aluminium can also be used as a structural material but its foaming at ambient conditions is not possible due to its high reactivity. A separate shielding gas environment is to be created while foaming magnesium [4, 5]. Aluminium eliminates the disadvantages that both magnesium and titanium possess and thus can be used as a suitable foaming material for structural applications but its compressive strength is low so efforts to increase its compressive strength are required [4, 5].

Aluminium foams are excellent impact energy absorbers, and they can convert impact energy into deformation energy and absorb more energy than bulk metal at low stress [5]. The long plateau behaviour of the stress-strain curves of aluminium foams makes them ideal materials for energy absorption. Aluminium foam-filled tubes have been examined for energy absorption and results have shown that due to the interaction effect between tube and filler, the foam-filled tube formed more folds, and foam filler formed one new extreme densification region, which resulted in the longitudinal compressive load and energy absorption value of foam filled tube much higher than the sum of foam and tube [4, 5].

4.2 Selection of Blowing Agent

From the above discussion, it was found that mainly carbonates and hydrides are used as blowing agents. However, as a foaming agent for the production of aluminium alloy foams by the casting and powder metallurgical routes, TiH_2 has several limitations that significantly influence the mass application of Al foams [4, 5]. The main limitations of foaming technologies using TiH_2 as the foaming agent are the following [4, 5, 8]:

- TiH_2 is expensive making such production less competitive.
- The decomposition temperature of TiH_2 is very low – starting at about 400°C for the untreated hydride – and commercial aluminium alloys have a solidus temperature above 525°C. Untreated TiH_2 does not match well the melting range of any of the Al alloys applied for foaming.
- Pre-treatment of TiH_2 by oxidation, which covers the surface of TiH_2 particles with a TiO_2 layer, or other surface engineering techniques for creating specific protective layers was found to shift the decomposition range to higher temperatures. Although these procedures work well they increase the cost.
- TiH_2 particles act only as the blowing agent and are not involved in foam stability; Therefore, if TiH_2 is applied, the addition of other solid particles (e.g., SiC) is necessary for bubble stabilization, which also introduces an extra cost.
- The density of TiH_2 (approx. 3.9 g/cm3) is significantly higher than the density of molten aluminium (approx. 2.7 g/cm^3). During foaming, the settling of TiH_2 particles occurs by gravity resulting in a non-uniform foam microstructure.
- A cost-effective and highly promising alternative to TiH_2 blowing agent is $CaCO_3$, as marble powder or synthetic calcium carbonate. In contrast to TiH_2, calcium carbonate has a low cost especially compared to aluminium, and with a density (2.71 to 2.83 g/cm^3) identical to the density of molten aluminium.
- Moreover, its decomposition temperature is above the melting point of aluminium, usually in the temperature interval between 660°C and 930°C.
- Therefore, $CaCO_3$ is particularly suitable for the melt-route settling-free production of foamed aluminium-based materials.

4.3 Research Gaps

- The high stiffness-to-weight ratio possessed by aluminium foam makes it an ideal material for use in several different applications, especially structural engineering.
- To use foams efficiently in any situation, it is essential to understand their behaviour and properties in scenarios relevant to potential uses.
- The level of accountability that exists in structural engineering projects and the catastrophic

repercussions of insufficient designs make this especially true.

- Foam properties are directly related to the relative density, whether the cells are open or closed, the degree of anisotropy of the foam, as well as the material properties of the ligaments [13].
- Aluminium foam possesses a high sound absorption capacity hence it can be used as a structural material for the construction of seminars and auditoriums where better communication is required.
- However, its low compression strength prevents its use in such areas so in this research work an effort has been made to increase the compressive strength of the aluminium foam.
- The final result obtained helps in deciding the best composition that has a good strength-to-weight ratio, and the highest energy absorption with uniform pores.
- The broad objective of the study is to evaluate the mechanical, wear, and physical performance of Al metal foam by adding Mn and Mg in different percentages for structural applications.

5 Methodology And Experimental Work

5.1 Experimental Setup

The experimental setup consists of the following main components. Assembled setup for foam manufacturing has been shown in Figure 1.

- **Crucible**: A standard A-4 graphite crucible was used for melting aluminium. Graphite crucible was used as it suited the temperature range also it has self-lubricating properties.
- **Crucible pit furnace**: The pit crucible furnace which is cylindrical consists of a grate inside on which coal and wood were placed for firing the furnace. The inside of the furnace was lined with fire bricks. A blower is attached to the furnace for providing a draft. A removal lid was placed on the furnace having a hole in the center with a diameter of 8 cm.
- **Stirrer**: Stirrer was indigenously built having two mild steel blades of 1.5 cm thickness. The length of the impeller shaft was 60 cm and it was attached to a 3-phase electric motor. To vary the speed of the motor a regulator was used.

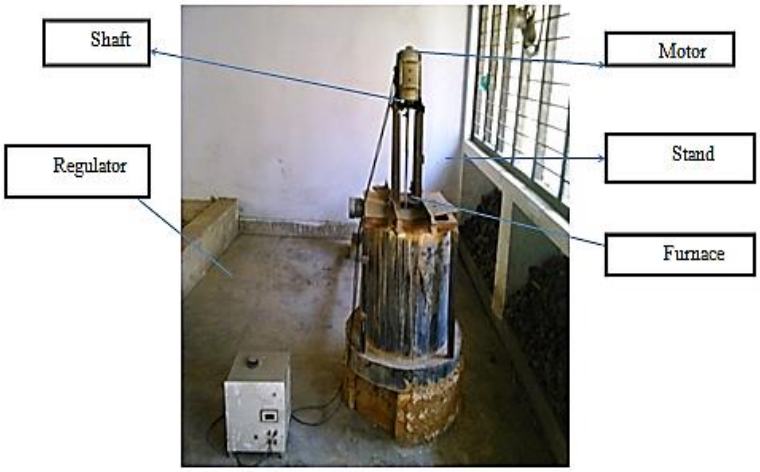

Figure1: Assembled setup for foam manufacturing

5.2 Sample Preparation

The procedure followed for foam manufacturing is explained in the following paragraphs (figure 2):

1. Firing the pit crucible furnace.
2. Place the crucible over the furnace and place solid pure aluminium (1 kg) in the crucible and then wait for it to melt.
3. Once aluminium melted the blower was switched off as too much high temperature makes the melt less viscous and thus hinders the foaming process
4. Calcium which acts as a viscosity-enhancing agent was then added (2 wt. % of aluminium). The calcium was added to the powder foam.
5. Then stirring was initiated at around 200 rpm for about 2 minutes so that calcium gets mixed with molten aluminium and makes the melt viscous.
6. After calcium Mn was added to molten aluminium in 1.5 wt. %.Then stirrer was placed on the furnace and stirring was initiated.

7. The stirring speed was 200 rpm and was done for 2 minutes.
8. Afterwards, Mg was added in different weight percentages (0, 0.5, 1, and 1.5 wt. %) and stirred for the next 2 minutes.
9. After that calcium carbonate was added (1 wt. %) and again stirring was done at the speed of 200 rpm for 2 minutes.
10. The stirrer was removed and a holding time of about 10 sec was provided which resulted in the foaming of the aluminium inside the crucible.
11. Then crucible was removed from the furnace and kept in the air so that the foamed molten metal may cool down.
12. After the removal of the foam from the crucible sample of a specified size was cut from it for the desired testing.

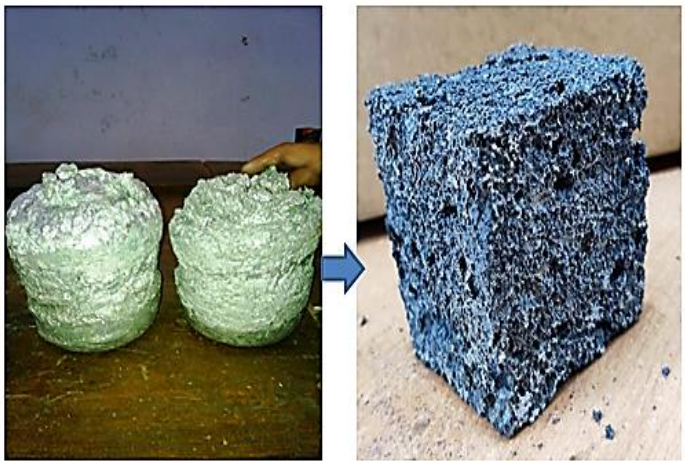

Product drawn out of Crucible Final Product

Figure 2: Aluminium foam prepared for experimental work

Prepared samples are cut and used for testing purposes by their suitable names. The designations with the detailed composition are tabulated below in Table 2.

Table 2: Sample designation

Sample Designation	Composition		
	Al (wt%)	Mn (wt%)	Mg (wt%)
Foam-0	100	0	0
Foam-1	97.5	1	1.5
Foam-2	97	1	2
Foam-3	96.5	1	2.5

5.3 Mechanical Properties of Aluminium Foam

- Density: A measuring jar was used to determine the metal foam's density. To find density [19, 26], take the weight of the specimen in the air. Fill the jar with water at a certain level and record it. Now submerge the sample in it; a slight increase in the water level will occur, which needs to be noted. The rise in the volume of water in the jar is the volume of the specimen. Now apply the standard formula for calculating the density as per equation (6).

$$\rho_{foam} = \frac{m}{v} \quad (6)$$

- Porosity Percentage: Porosity is the ratio of pore density to bulk material density for a given volume. The porosity of foams was evaluated by the following equation (7) [19, 26]:

$$\text{Percentage of porosity} = \frac{\rho_{al} - \rho_{foam}}{\rho_{al}} \quad (7)$$

- Macrostructure Evaluation: Using a digital camera with good pixels, the macrostructure of the metallic foam samples was analyzed. The pictures of the specimens were taken to examine the pores' size,

irregularity, and distribution. The size of pores can also be determined given by equation (8) [19, 26]:

$$D = {}^{L}/_{0.616} \quad (8)$$

Where D and L are the average diameter and chord length of polyhedron pores.

- Scanning electron microscope test: A scanning electron microscope (SEM) was used to look at the aluminium foam pore size. SEM is a very useful tool for the non-destructive inspection, analysis, and evaluation of metallic and non-metallic materials.
- Compression test: For the compression test specimens of size, 30 x 30 x 30 mm were prepared. The specimen was kept on the bed of the machine and the ram was allowed to apply load on the specimen. Once the specimen started to get deformed. The load applied was in KN while the displacement was measured in mm. Compression tests were performed on a Heico electronic universal testing machine having a capacity of 400kN and 200mm ram stroke.

6 Results And Discussions

6.1 Composition of Various Aluminium Foams

6.1.1 Form-0 (pure aluminium)

Figure 3 shows a typical cross-section image of cellular Al foam. It can be seen that the pore structure is homogeneous except for one or two relatively larger pores and the pores are depicted.

Figure 3: Cross-section of pure aluminium foam

Figure 4 represents the cell structure of the foamed sample. Small pores are present inside the cell wall of larger pores. The average pore size of aluminium foam is around 1-3mm. The average pore size obtained in the experimental work is 1.6mm. The density of the foam was found to be around 0.52 gm/cm^3.

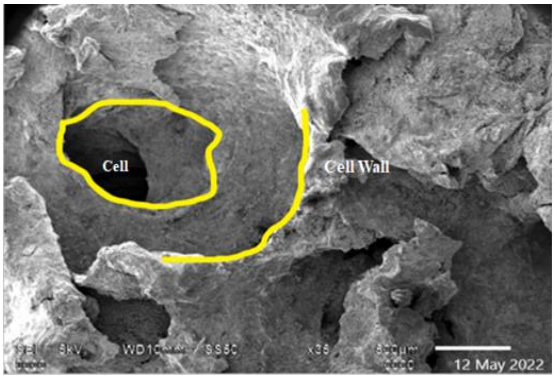

Figure 4: SEM image of pure aluminium foam

The large pores are attained due to unstable bubble formation. The border's strength decreases with the reduction in plateau border thickness. Due to this, the border can no longer withstand the pressure coming from inside, and eventually, the cell wall breaks, causing the pores to enlarge. A thickening agent acts as a key element and prevents bubble enlargement.

6.1.2 Foam-1 (Al +Mn 1%+Mg 1.5%)

Foam-1 has a density of 0.614gm/cm^3. Figure 5 represents the optical image where pores are uniformly distributed and most of them are of uniform size. It is very tough to control the foaming in all of the places in the matrix. So the formation of the pores looks satisfactory.

Figure 5: Cross-sectional image of foam-1

The SEM image is represented in Figure 6. The image represents the distribution of reinforcing particles, which are connected close to each other. The solid white grains and some sponges-type structures are distributed in a grey matrix. It means that Mg particles helped the bonding to become strong. It represents the importance of Mg particles in the matrix. It supports the previous research that identified Mg as an element assisting the bonding between the parent metal and the reinforcing agent [31, 33].

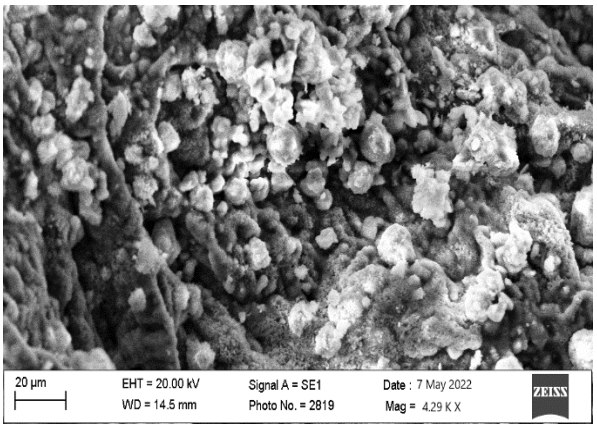

Figure 6: SEM image of foam-1

6.1.3 Foam-2 (Al +Mn 1%+Mg 2%)

The density of foam-2 was found to be 0.48gm/cm^3. The pores seen in Figure 7 look uniform and of equal size, except in some of the places. The size of small pores is 1mm-2mm, but big size pores are 4mm-5mm big.

Figure 7: Cross-sectional images of foam-2

The pores are found almost uniform at the periphery while looking at the centre of the optical image, it is found that the pores are unevenly distributed and are of larger size. It can be predicted that during the removal of the stirrer from the melt, the layer of thickening agent got broken, causing the pores to enter their death phase. The SEM image of foam-2 in Figure 8 shows some small cells as represented by a yellow curve. These cells have a polygonal shape. It represents the significance of the thickening agent which helps in creating electrostatic forces that prevent a foam film from collapsing, the thickening agent helps form a dense mono-layer on a cell wall.

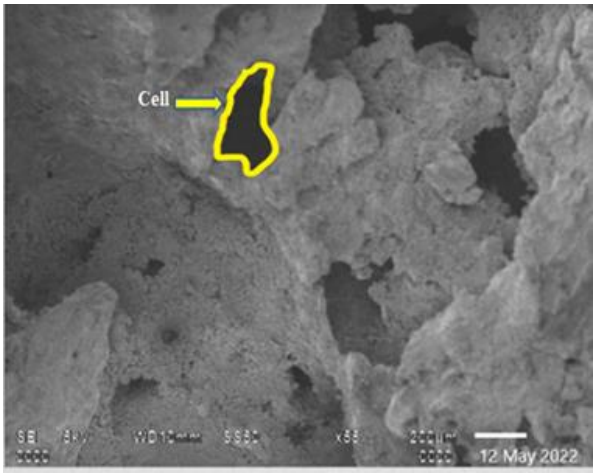

Figure 8: SEM image of foam-2

6.1.4 Foam-3 (Al +Mn 1% + Mg 2.5%)

The density of foam-3 is 0.5gm/cm^3. The optical image of foam-1 is depicted in Figure 9. Pores of various sizes are formed. The size of the pores are varying between 2mm and 3mm as calculated by the formula. It can also be observed that the pores are formed somewhere in a non-uniform pattern and in some places, there is no pore formation. The bigger pores are also found at the edges of the sample. These are obtained due to unstable bubble formation. It can also be seen that some blowing agent is also present in the pores. It means that there is improper mixing. In the optical image of foam, a layer over the pores gets cemented due to which the pores become invisible.

Figure 9: Optical image of foam-3

The SEM image in Figure 10 shows that during the formation of bubbles, some of the walls are missing. The cell grows larger due to these missing cell walls as depicted at the edges of figure 10. It was understood by the SEM image and it was found that the pores were generated properly but the gaps were filled by the accumulation of precipitants. The particles mixed and segregated between the missing walls. The reason can be the melting point of Mn which is 1246^0C. With the addition of Mg in higher percentage viscosity got increased and Mn did not get any sufficient heat energy to distribute throughout the melt. Hence the elements do not participate in the reaction and get deposited between the walls.

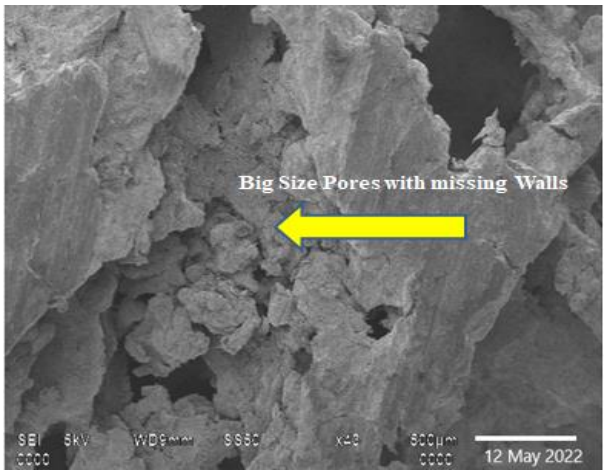

Figure 10: SEM image of foam-3

Figure 11 shows the comparison of stress and strain for all four foams under experimentation. The energy absorption of foams is calculated by calculating the area under the stress-strain curve. It is found that foam-0 has the lowest value of energy absorption and with the addition of reinforcement; the value of energy absorption increases for all the cases.

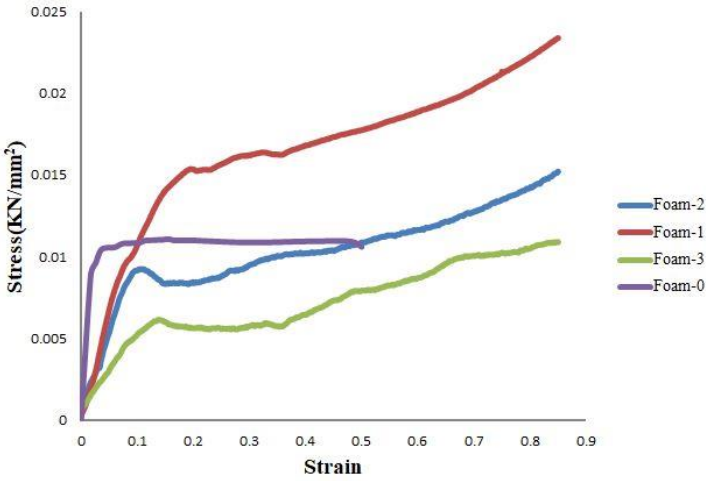

Figure 11: Comparative stress-strain curve of foams

The results of the density, foaming efficiency, yield strength, strength-to-weight ratio, and energy absorbed for all four samples of aluminium foams are tabulated in Table 3.

Table 3: Experimental test results

Sr	Foam	Density (g/cm^3)	Foaming efficiency (%)	Yield strength (MPa)	Strength-to-weight ratio	Energy Absorbed (MJ/m^3)
1	Foam-0	0.52	80.52	9.63	18.5	5.24
2	Foam-1	0.614	79	15.34	24.98	22.748
3	Foam-2	0.48	82	8.95	18.64	14.14
4	Foam-3	0.5	81.3	5.42	10.84	9.56

Foam-0 has good yield strength but cannot produce a longer plateau. The total energy absorbed up to the plateau is 5.24 MJ/m^3. Foam-1 displays the longest and smoothest plateau region of all the curves. Moreover, the value of collapse stress is also maximum. It has been already discussed in the study that the extent of each region is a function of density. The density of foam-1 is 0.614 g/cm^3. The value of energy absorption calculated by software is 22.75 MJ/m^3. Which is about 4 times foam-0. Looking towards the length of the plateau of foam-1, it is found that the length reaches up to 0.9 strain. It seems to be the potential reason behind the energy absorption.

In this region, deformation begins in the weakest area and spreads to the stronger area until the entire area is crushed. In succeeding bands, this procedure is repeated. The compressive stress of the foam remains essentially constant because each band has nearly the same strength. The ability of foam to absorb energy is largely a result of the cell walls' yielding, buckling, and friction [36]. The proper distribution of the Mn and Mg elements in Foam-1's cell wall matrix and the thickening agents along the cell wall edges support the material's ability to resist deformation. It is found experimentally that with an increase in the percentage of Mg element in the melt, the energy absorption increases enormously.

In the study of foam-2, it was found that the value of collapsible stress reduces dramatically but the length of the plateau remains longer. The value of energy absorption is found to be 14.14 MJ/m^3. Which drops significantly in comparison to foam-1.The addition of 2wt. % Mg in the melt is showing a detrimental effect but still gives a comprehensive value of energy absorption. The study of foam-3 exhibits a substantial drop in collapsible stress and the plateau region looks interrupted. The plateau region shows dual nature. It exhibits the plateau and densification region simultaneously. The value of energy absorption calculated is 9.56 MJ/m^3.

Among all the foams, foam-0 has the shortest plateau. With the addition of Mn and Mg in the melt the length of the plateau increases. It emphasizes the need for reinforcing elements in the melt to perform solid solution strengthening. With the addition of Mg above 1.5wt. %, it is found that the value of yield strength and energy absorption decreases. The accumulation of precipitants in cell walls and pores' non-uniformity seems to be an appropriate reason behind this decline.

6.2 Comparison based on Measured Properties

6.2.1 Based on the compression behaviour of foams

It has been found previously, that foam-1 has the highest compressive value. But on the other hand, considering the density, foam-1 has the maximum value of density i.e., 0.614 gm/cm^3. It should be noted that due to the addition of Mn (1 wt. %) and Mg in varying percentages, initially, the compressive strength increases, and then finally for Mg (for 2 and 2.5 wt. %) the compressive strength of the foam decreases.

For metallic foam, the first peak stress on the stress-strain curve is defined as yield strength. From compressive stress-strain diagrams, it is inferred that the yield strength of Foam-1 is higher than pure Al foam (foam-0) and the strength-to-weight ratio also increases. It means that the addition of Mn and Mg initially shows significant improvement in the mechanical properties of aluminium foam. The possible reason behind this is the proper mixing of reinforcing particles. In the case of foam-2 the density of foam decreases and yield strength reaches about equal to foam-0. The strength-to-weight ratio shows that foam-2 performs better than foam-0. Foam-3 represents the lowest yield strength and lowest strength-to-weight ratio. Calculating yield strength/density, it has been found that the values foam-0: foam-1: foam-2: foam-3 are in the ratio of **1: 1.35: 1.007: 0.59.** So from this point of view foam-1 has the highest compressive strength.

6.2.2 Based on the energy absorption of foams

It is found from the experiments that foam-1 produces the highest value of energy absorption and reduces with the further addition of Mg particles. The area under the stress-strain curve was found to be maximum for foam-1. As foam-0 densifies about 0.5 strain it produces minimum energy. Foam-1, 2, and 3 have a longer plateau respectively. The addition of reinforcement helped in increasing the length of the plateau.

The comparison shows that foam-1 exhibits maximum energy. So for structural applications, foam-1 was found suitable as an energy absorber. Due drop in the density of foam-2 and foam-3 and non-uniformity in cell size and distribution reduces the performance of these foams. Figure 11 shows the graph of the comparison of stress and strain among foam-1, foam-2, and foam-3 respectively. It is clear from the graph in Figure 11 that at the high value of stress, foam-1 is highly stable and exhibits higher strain. It means that foam-1 has the highest capacity to withstand high pressure and forces without failure. This advocates the selection of foam-1 as the best foam among all four foams.

6.2.3 Based on the microstructural behaviour of foams

Foam-0 produces a uniform structure. Foam-1 also shows a satisfactory structure, except in some of the places. Foams-2 & 3, on the other hand, have higher porosity, allowing them to make thinner cell walls. The compression strength of foam solely depends only on porosity [32]. This implies that the higher the foam porosity, the weaker the cell wall. Hence unable to withstand a higher load and have a lower compression strength value. By increasing the percentage of Mg further in the melt the porosity increases, reducing the thickness of the cell wall and showing depreciation in the value of yield and energy absorption.

From this discussion, it is found that Foam-1 shows uniformity in the pores and produces the lowest porosity. The distribution of pores allows it to produce a longer plateau as well. So foam-1 is found to be superior among all other foams based on pores morphology. Figure 12 shows the comparison of the performance parameter of foams as depicted in Table 3.

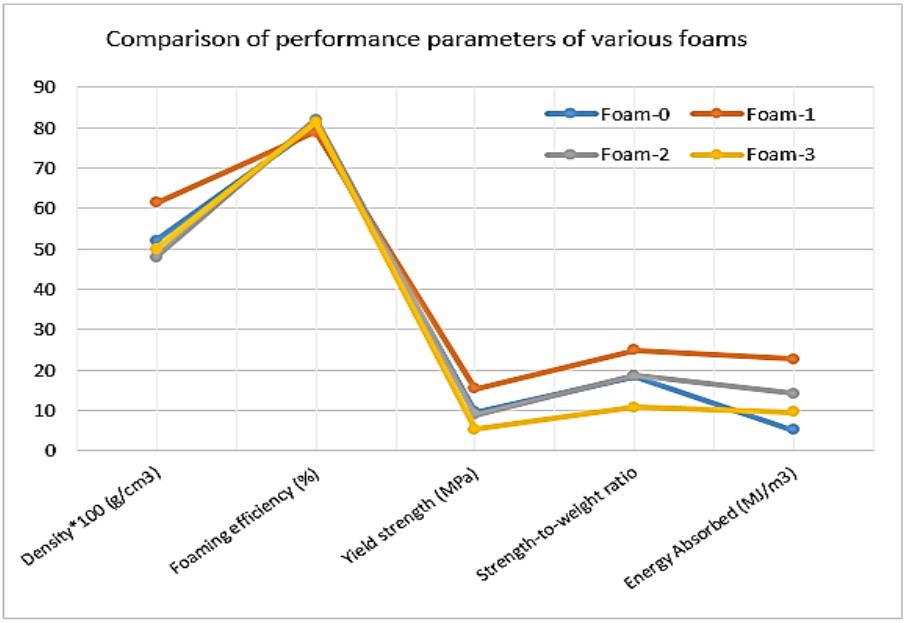

Figure 12: Comparison of performance parameters of various foams

7 Conclusions and Future Scope

Closed-cell aluminium foams with the addition of Mn (1 wt.%) and Mg (1.5, 2, and 2.5) were successfully prepared by the melt route method. In the process, Ca was used as a thickening agent and $CaCO_3$ as a foaming agent. The effect of reinforcing elements on the morphology and mechanical behaviour of Al-based metal foam was studied. From the current work, it is inferred that the addition of reinforcing elements initially helped to increase the compressive strength as found in foam-1, but further addition of Mg did not have any beneficial effects. The value of compression strength depends on foam density.

From the optical images, it is observed that pure Al foam has uniform pores. With the addition of reinforcing particles, the pore distribution, and size change. Foam-1 shows satisfactory results but foam-2 and foam-3 pores had detrimental effects. From the evaluation, it can be concluded that besides the increase in density and variations in pores uniformity Foam-1 was found to be superior among all other foams. It can also be concluded that by fixing the percentage of Mn (1 wt%), the best results can be obtained by adding Mg by 1.5 wt.% in the melt. Further addition of Mg shows a detrimental effect on mechanical and physical properties.

In future, more research is required to create foam with uniform pore size. It is necessary to have accurate knowledge of the foaming temperature. This is because preventing the coalescence phase of the foaming process, which is dependent on the controlled foaming temperature, is the only way to achieve uniform pore size. Therefore, the correct understanding of temperature distribution is required. Additionally, to consistently obtain sound foam, the entire melt route process needs to be optimized. This can be done by choosing the appropriate exposure of blowing agent, thickening agent, stirring rpm, stirring time, and holding time.

Bibliography

[1] J. Banhart. 2001. Manufacture, characterization, and application of cellular metals and metal foams. Progress in Materials Science 46(6): 559-632.

[2] B. Smith, H. Bastawros, A. Mumm, D.R. Evans, D.J. and Wadley. 1998. Compressive deformation and yielding mechanisms in cellular al alloys determined using x-ray tomography and surface strain mapping. Acta Materialia 46(10): 3583-3592.

[3] C.S. Marchi and A. Mortensen. 2004. Deformation of open-cell aluminium foam. Acta Materialia 52: 2895–2902.

[4] B. Matijasevic-Lux, J. Banhart, S. Fiechter, O. Gorke and N. Wanderka. 2006. Modification of titanium hydride for improved aluminium

foam manufacture. Acta Materialia 54: 1887–1900.

[5] J. Banhart. 2005. Aluminium foams for lighter vehicles. International Journal of Vehicle Design 37(2/3): 114-125.

[6] L.J. Gibson and M.F. Ashby. 2000. Cellular solids: structures and properties. Cambridge: Cambridge University Press.

[7] Baumgärtner, F. Duarte and J. Banhart. 2000. Industrialization of powder compact foaming process. Advanced Engineering Materials 2(4): 168-174.

[8] T. Koizumi, K. Kido, K. Gnyloskurenko and T. Naamura. 2012. Method of preventing shrinkage of aluminium foam using carbonates. Metals 2(1): 1-9.

[9] J. Banhart. 2008. Manufacturing routes for metallic foams. The Journal of The Minerals, Metals & Materials Society 52(12): 22-27.

[10] J. Kováèik. 2004. Comparison of zinc and aluminium foam behaviour. Kovove Materialy 42(2): 79-90.

[11] Z. Esen and S. Bor. 2007. Processing of titanium foams using magnesium spacer particles. Scripta Materialia 56(5): 341-344.

[12] M. Haesche, D. Lehmhus, J. Weise, M. Wichmann and I.C.M. Mocellin. 2010. Carbonates as foaming agent in chip-based aluminium foam precursor. Journal of Materials Science and Technology 26(9): 845-850.

[13] T.R. Neu and M. Mukherjee, F. Garcia-Moreno and J. Banhart. 2011. Magnesium and magnesium alloy foams. International Conference on Porous Metals and Metallic Foams: 133-140.

[14] L.E.G. Cambronero, J.M. Ruiz-Roman, F.A. Corpas and J.M.R. Prieto. 2009. Manufacturing of Al-Mg-Si alloy using $CaCO_3$ as foaming agent. Journal of Materials Processing Technology 209(4): 1803-1809.

[15] D. Li, J. Li, T. Li, T. Sun, X. Zhang, G. Yaol. 2011. Preparation and characterization of aluminium foams with ZrH2 as foaming agent. Transactions of Nonferrous Metals Society of China 21(2): 346-352.

[16] V. Kevorkijan. 2010. Low-Cost Aluminium foams made by CaCO3 particulates. Association of Metallurgical Engineers of Serbia 16(3): 205-219.

[17] M. Tajally, Z. Huda and H.H. Masjuki. 2009. Effect of cold rolling on bending and tensile behaviour of 7075 aluminium alloy, Journal of Applied Sciences 21(9): 3888-3893.

[18] A.V. Byakova, S.V. Gnyloskurenko, A.I. Sirko, Y.V. Milman and T. Nakamura. 2006. The role of foaming agent in structure and mechanical performance of Al-based foams. Materials Transactions 47(9): 2131-2136.

[19] N. Onsalung, C. Thinvongpituk and K. Painthong. 2010. The Influence of foam density on specific energy absorption of rectangular steel tubes. Energy Research Journal 1(2): 135-140.

[20] L.D. Kenny. 1996. Mechanical properties of particle stabilized aluminium foam. Materials Science Forum 217-222: 1883-1890.

[21] Z. Hussain and N.S.A. Suffin. 2011. Microstructure and mechanical behaviour of aluminium foam produced by sintering dissolution process using NaCl space holder." Journal of Engineering Science 7: 37–49.

[22] K. Mohan, T.H. Yip, I. Sridhar, Z. Chen. 2011. Impact response of aluminium foam core sandwich structures. Materials Science and Engineering A 529: 94–101.

[23] M. Shiomi and Y. Tanino. 2011. Moulding of aluminium foams by using hot powder extrusion. Metals - Open Access Metallurgy Journal 2(2):136-142

[24] I. Paulin, B. Sustarsic, V. Kevorkijan, S.D. Skapin and M. Jenko. 2011. Aluminium foams production by powder metallurgy process. Materials and Technologies 45(1):13-19.

[25] V. Crupi, G. Epastoemail and E. Guglielmino. 2011. Impact response of aluminium foam sandwiches for light-weight ship structures. Metals 1(1): 98-112.

[26] S. Haidar, J. Ghose, G. Sutradhar. 2015. Synthesis and compressive characterization of aluminium-SiCp composite foam by stir-casting technique using dual foaming agent. International Journal of Advanced Information in Engineering & Technology 8(8): 11-17.

[27] J. Ghosh, V. Sharma and S. Kumar. 2011. Al-MMC foam: synthesis and characterization. Journal of Materials and Metallurgical Engineering 1(1): 1-10.

[28] B. Matijasevic-Lux, J. Banhart and S. Fiechter, O. Görkea and N.Wanderkab. 2006. Modification of titanium hydride for improved aluminium foam manufacture. Acta Materialia 54(7): 1887-1900.

[29] C.S. Marchi and A. Mortensen. 2001. Deformation of open-cell aluminium foam. Acta Materialia 49(19): 3959–3969.

[30] B.H. Smith, S. Szyniszewski, J.F. Hajjar. B.W. Schafer, S.R. Arwade. 2012. Characterization of steel foams for structural components. Metals 2: 399-410.

[31] J. Banhart. 2006. Metal Foams: Production and Stability. Advanced Engineering Materials 8(9): 781–794.

[32] Y. Hangai, S. Koyama, M. Hasegawa and T. Utsunomiya. 2010. Fabrication of aluminium foam/dense steel composite by friction stir welding. Metallurgical and Materials Transactions A 41: 2184-2186.

[33] A. Li, H. Xu, L. Geng, B. Li, Z. Tan, W. Ren. 2012. Preparation and characterization of SiCp/2024Al composite foams by powder metallurgy. Transactions of Nonferrous Metals Society of China 22(1): s33–s38.

[34] Y. Zhou, Z. Chuan Hong, Xiang Ping Ai, Xiao Qing Zuo. 2013. Manufacture, structure and properties of copper foams. Advanced Materials Research 652-654: 1163-1166.

[35] X. Xia, H. Feng, X. Zhang and W. Zhao. 2013. The compressive properties of closed-cell aluminium foams with different Mn additions. Materials & Design 51: 797–802.

[36] D. Yang, S. Guo, J. Chen, J. Lu, L. Wang, J. Jiang and A. Ma. 2018. Fabrication of Cu-Mg alloy foam with close pore structure by gas release reaction powder metallurgical approach. Journal of Alloys and Compounds 766: 851-858.

[37] J. Liu, Q. Qu, Y. Liu, R. Li and B. Liu. 2016. Compressive properties of Al-Si-SiC composite foams at elevated temperatures. Journal of Alloys and Compounds 676: 239-244.

[38] S. Kumar and O.P. Pandey. 2015. Study of microstructure and mechanical properties of particulate reinforced aluminium matrix composite foam. In: T. Sano and T.S. Srivatsan (eds) Advanced Composites for Aerospace, Marine, and Land Applications II: 245-257.

[39] H. Choi, S. Shil'ko, J. Gubicza and H. Choe. 2017. Study of the compression and wear-resistance properties of freeze-cast Ti and Ti–5W alloy foams for biomedical applications. Journal of the Mechanical Behaviour of Biomedical Materials 72: 66-73.

[40] A. Bisht and B. Gangil. 2018. Structural and physico-mechanical characterization of closed-cell aluminium foams with different zinc additions. Science and Engineering of Composite Materials 25(4): 789-795.

[41] A. Bisht, B. Gangil and V.K. Patel. 2019. Physico-compression, sliding wear and energy absorption properties of Zn/Mg infiltrated closed cell aluminium foam. Materials Research Express 6(10): 1-17.

[42] M.H. Ghaleh, N. Ehsani and H.R. Baharvandi. 2021. High-porosity closed-cell aluminium foams produced by melting method without stabilizer particles. International Journal of Metal Casting 15: 899-905.

[43] http://materialsscience.org/amray-3200-sem-eds/ (assessed on July 08, 2023).